J Sol-Gel Sci Technol (2018) 85:431–435
DOI 10.1007/s10971-017-4549-y

ORIGINAL PAPER: SOL-GEL AND HYBRID MATERIALS FOR DIELECTRIC, ELECTRONIC, MAGNETIC AND FERROELECTRIC APPLICATIONS

Ferroelectric behavior of La and Mn co-doped $BiFeO_3$–$PbTiO_3$ thin films prepared by sol–gel method

Dongfang Chen[1] · **Jinrong Cheng**[2]

Received: 27 May 2017 / Accepted: 22 November 2017 / Published online: 30 November 2017

Abstract Solid solution films of $0.7BiFeO_3$–$0.3PbTiO_3$, $0.7(Bi_{0.97}La_{0.03})FeO_3$–$0.3PbTiO_3$, $0.7Bi(Fe_{0.96}Mn_{0.04})O_3$–$0.3PbTiO_3$ and $0.7(Bi_{0.97}La_{0.03})(Fe_{0.96}Mn_{0.04})O_3$–$0.3PbTiO_3$ on Pt/Si structures were fabricated by sol–gel process. Effects of La and Mn doping on microstructures, ferroelectric behavior and leakage current of $BiFeO_3$–$PbTiO_3$ films were investigated. It was found that the coercive field of the BLFPT thin films obviously reduced, owing to the enhancement of domain reversal by the incorporation of La ions. In contrast, Mn-doped films prefer to exhibit the improved polarization and decreased leakage current density. In order to combine the advantages of the two elements' doping, the films of binary elements co-substitution were successfully prepared. The La and Mn co-doped films demonstrated the best insulation compared with the other samples, which simultaneously achieved the optimized ferroelectric performance with the improved remnant polarization and reduced coercive field. The P_r and E_c values of co-doped $BiFeO_3$–$PbTiO_3$ thin films at room temperature were approximate 37 uC/cm^2 and 90 kV/cm, respectively.

Graphical abstract

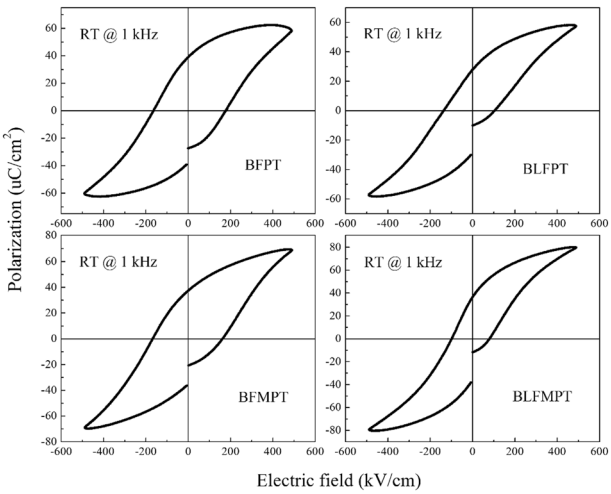

Keywords $BiFeO_3$–$PbTiO_3$ thin films · co-substitution · leakage · ferroelectricity

1 Introduction

Recently, The $BiFeO_3$(BFO)-based thin films have been widely studied as an substitute to $Pb(Zr_xTi_{1-x})O_3$ (PZT) films, owing to their environment-friendly features and outstanding performance. These materials exhibit multiple order parameters (charge, spin) simultaneously in the same phase, which made it possible for the application of non-volatile memories and spintronic devices [1–3]. In the family of $BiFeO_3$-based films, $BiFeO_3$–$PbTiO_3$(BFPT) binary system demonstrate the decreased coercive field and

✉ Jinrong Cheng
jrcheng@staff.shu.edu.cn

[1] State Key Laboratory of ASIC and System, School of Microelectronics, Fudan University, Shanghai 200433, PR China

[2] School of Materials Science and Engineering, Shanghai University, Shanghai 200444, PR China

improved remnant polarization in the region of the MPB compared with BFO films, making it a promising candidate for data storage [4, 5]. Unfortunately, even with a more stable structure, the BFPT thin films still exhibit a high leakage current at room temperature (RT). Sakamoto et al. [5] clarified the low insulating resistance of BFPT films synthesized on $Pt/TiO_x/SiO_2/Si$ substrates by chemical solution deposition (CSD), although their leakage current density decreased with the increase of $PbTiO_3$ content.

Numerous attempts have been devoted to overcome this shortcoming, which include introduce appropriate buffer layer [6–8], construct a multilayer structure [9, 10] and A/B site substitutions [11–16]. By comparison, ions substitutions have been proved to be an effective way in reducing the leakage current in BFO-based thin films. Kim et al. [12] demonstrated the reduced leakage current density of 20 mol % La substitution in epitaxial $BiFeO_3$ thin films. Subsequently, Sakamoto et al. [5] confirmed the enhanced insulation of $BiFeO_3$–$PbTiO_3$ films via Mn doping but no saturated P–E hysteresis loops were addressed in RT [5]. However, a degradation of ferroelectric behavior often to be found in the BFPT ceramics with La incorporation and Mn doping may cause trouble for domain switching inside the ferroelectric films. Therefore, in this paper, we propose a new combination of La and Mn as co-doping elements in $BiFeO_3$–$PbTiO_3$ thin films, which may allow overall improvements of ferroelectric properties.

2 Experimental procedures

$0.7BiFeO_3$–$0.3PbTiO_3$ (BFPT), $0.7(Bi_{0.97}La_{0.03})FeO_3$–$0.3PbTiO_3$ (BLFPT), $0.7Bi(Fe_{0.96}Mn_{0.04})O_3$–$0.3PbTiO_3$ (BFMPT) and $0.7(Bi_{0.97}La_{0.03})(Fe_{0.96}Mn_{0.04})O_3$–$0.3PbTiO_3$ (BLFMPT) thin films were prepared on Pt/Si substrates by sol–gel technique. As the starting materials, the analytically pure $Bi(NO_3)_3{\cdot}5H_2O$, $Fe(NO_3)_3{\cdot}9H_2O$, $Pb(CH_3COO)_2$, $Ti(OC_3H_7)_4$, $La(NO_3)_5{\cdot}xH_2O$, $Mn(CH_3COO)_2{\cdot}4H_2O$ were dissolved in 2-Methoxyethanol for the preparation of precursor solution. In order to compensate the evaporation of Pb and Bi during annealing, $Pb(CH_3COO)_2$ were 10 mol% excess and $Bi(NO_3)_3{\cdot}5H_2O$ were 2 mol% mol excess. The final concentration of precursor solution was 0.4 mol/L. The stoichiometric solutions were spin-coated for 30 s with the speed of 3500 rpm, then the samples were dried at 200 °C for 3 min, calcined at 300 °C for 2 min and at 500 °C for 4 min by rapid temperature annealing. The process of coating and calcination cycle were repeated 8 times until obtain approximately 600 nm thick films which then were annealed at 600 °C for 30 min in the air. Circular Pt top electrode with a radius of 2 mm were deposited on the BFPT films by magnetron sputtering through a shadow mask. The phase structures of the films were characterized by X-ray diffraction (XRD) system (Rigaku D/Max-2200 V, Japan) using Cu Ka radiation. A field-emission scanning electronic microscope (FESEM, JEOL, JSM-7000F, Japan) was used to examine the microstructures. The leakage current density and the electric hysteresis loops of the thin films were characterized by a ferroelectric test system RT6000HVS (Radiant Co.).

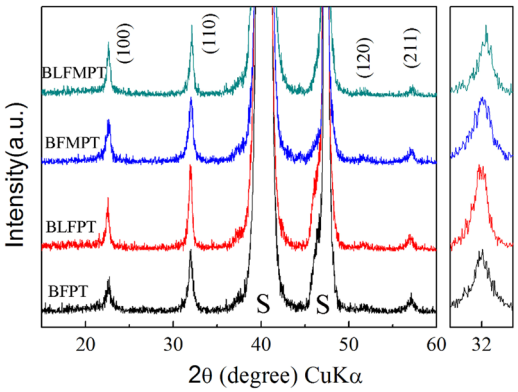

Fig. 1 XRD patterns of BFPT, BLFPT, BFMPT and BLFMPT thin films (Pt-underlayer reflections are marked with S)

3 Result and discussion

The XRD patterns of BFPT, BLFPT, BFMPT and BLFMPT thin films fabricated on Pt/Si substrates are shown in Fig. 1. All of the films exhibit a single-phase perovskite structure, with no secondary phase addressed. It is found that BLFPT tend to display a sharp and stronger single peak at $2\theta = 32°$, indicating the positive effect of La substitution in promoting the process of crystallization. Meanwhile, the film of BFMPT exhibits no obvious change except for the insignificant enhancement of peak intensity at $2\theta = 22.5°$. The diffraction peak of BLFMPT demonstrates the both features of BLFPT and BFMPT films. Specifically, the FWHM of (100) and (110) plane of the BLFMPT thin film decreases slightly when compares to the pure BFPT film, and it simultaneously exhibit a slightly enhanced peak in (100) plane. It is believed that the change revealed from diffraction peak indicate the BLFMPT film could simultaneously demonstrates the both advantages of BLFPT and BFMPT films.

Figure 2 shows FESEM images of BFPT, BLFPT, BFMPT and BLFMPT thin films prepared on Pt/Si substrates. The surface morphology displayed in the images tend to be smoother in Fig. 2b. The image of BFMPT film in Fig. 2c fails to show a significant change apart from the roughness is a little higher than BFPT film, which may give rise to the formation of inhomogeneous domains [2]. It is found from the Fig. 2d that the BLFMPT thin film

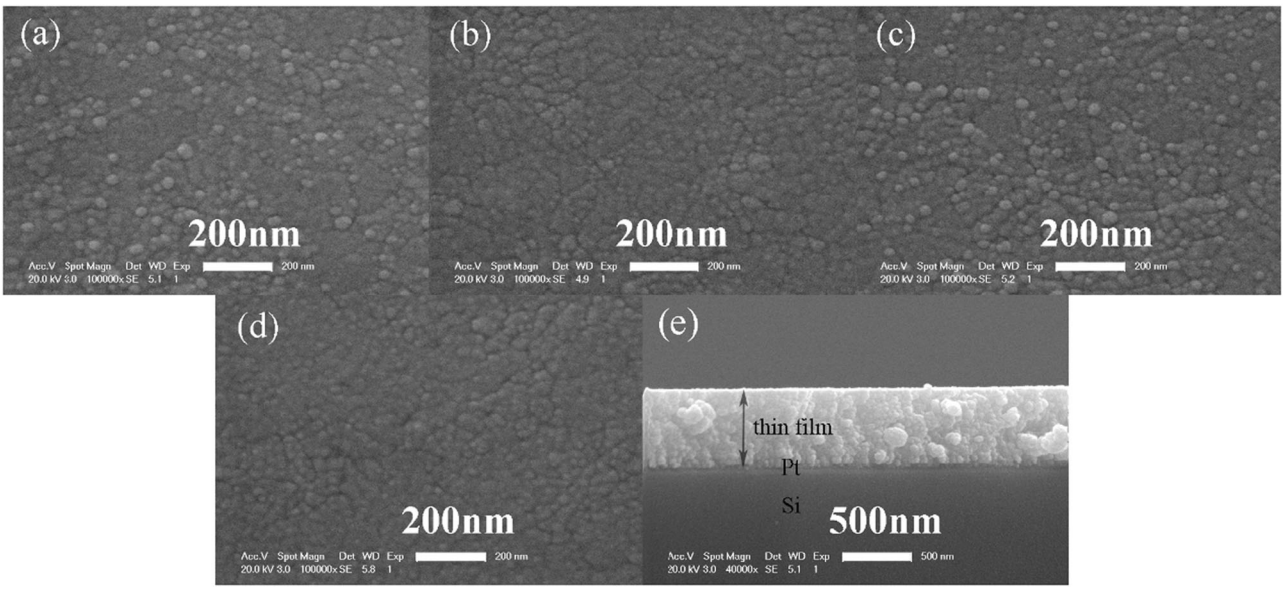

Fig. 2 FESEM images of surface morphologies of **a** BFPT, **b** BLFPT, **c** BFMPT and **d** BLFMPT thin films; **e** A typical FESEM cross-sectional image of the films

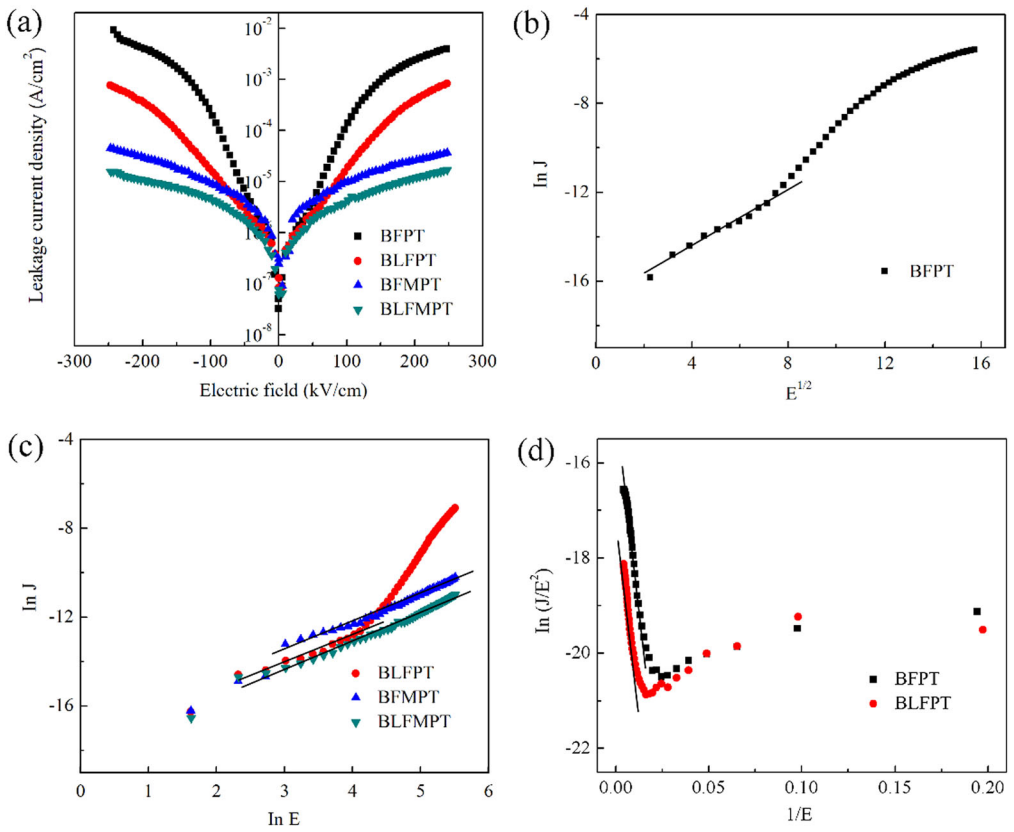

Fig. 3 Leakage currents of BFPT, BLFPT, BFMPT and BLFMPT thin films plotted with **a** J vs. E, **b** ln J vs. $E^{1/2}$, **c** lnJ vs. lnE, and **d** ln(J/E^2) vs. 1/E

demonstrates the smooth surface morphology and uniform grain size distribution by the La incorporation. The smooth surfaces often reflect the more homogeneous domains and reduced domain wall density in the films, which could contribute to the reduced leakage current and improved ferroelectric behavior [17].

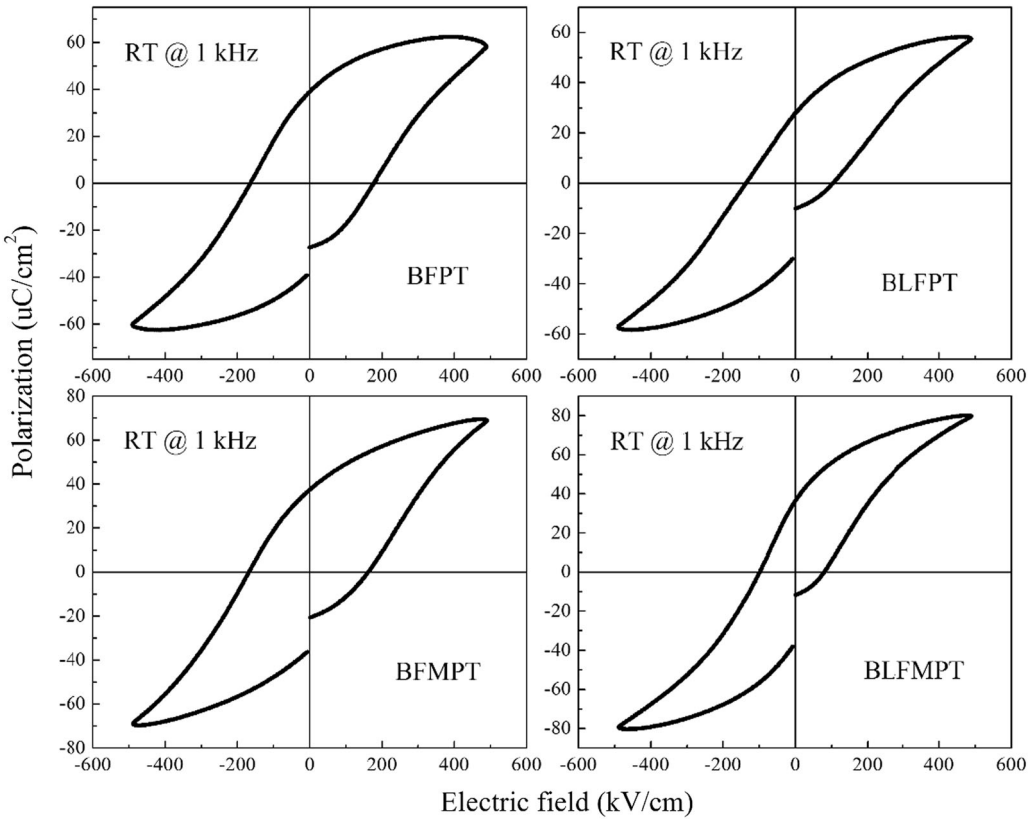

Fig. 4 P–E loops of BFPT, BLFPT, BFMPT and BLFMPT thin films

Figure 3a shows I-V characteristics of BFPT, BLFPT, BFMPT and BLFMPT thin films fabricated on Pt/Si structures measured at RT. Improvement of the symmetry of the J–E curves is found with the substitution of La or Mn ions, indicate the conduction mechanism changes from interface-limited to bulk-limited. Simultaneously, La and Mn doping also exhibits disparate leakage behavior in the measured electric field region. It is found that the La-doped BFPT film exhibits a lower leakage current than those of BFPT compositions in a low applied field range. On the contrary, the film of BFMPT tend to demonstrate reduced leakage density in the high electric field region and a higher leakage current is found in the lower electric field range [5]. La and Mn co-substitution is proved to be able to acquire a comprehensive reduction of leakage current, which is found in the BLFMPT films.

To clarify the conduction mechanism in prepared films, the plots for $E^{1/2}$ vs. InJ for BFPT film in the applied field area of Fig. 3a are shown in Fig. 3b. Ferroelectric layer contacts with the metal layer may form a Schottky barrier at the interface, thus resulting in the current obeying interface-limited Schottky emission, in which the current density can be described as $J = AT^2 \exp\left(-\frac{\Phi - \sqrt{q^3 E/\pi\varepsilon_0\varepsilon}}{kT}\right)$ [18], where A is a constant, Φ is the barrier height, E is the electric field, ε_0 is the permittivity of free space, ε is the optical dielectric permittivity of thin film, k is Boltzmann's constant, and T is absolute temperature. Schottky emission is considered to be the dominant conduct mechanism in relatively low applied field area after a straight line fitting in Fig. 3b. The plots for In E vs. In J of the BLFPT, BFMPT and BLFMPT films are also displayed in Fig. 3c. Since the linear fitting with a slope of approximately 0.5 can be possible in the measured electric field, Ohmic conduction mechanism (the Ohmic conduction mechanism is evident from the linear conduction characteristic of $J \propto E$) is the predominant electric conduction in the BFMPT and BLFMPT films [12]. According to Singh et al.'s report, grains in the Mn-substituted films are more densely packed than other films. The improvement in the grain structure could be considered to be a major reason why the breakdown characteristics are improved by Mn substitution [13]. Meanwhile, for BLFPT thin film, Ohmic conduction was also observed in a low applied field range, then the conduction mechanism changed slightly when the electric field exceeds 55 kV/cm. Accordingly, The plots for $1/E$ in J/E^2 of the BFPT and BLFPT films are shown in Fig. 3d, which indicate that the predominant conduction mechanism of the BFPT and BLFPT films in relatively high applied field region is the Fowler–Nordheim tunneling process. It can be described as

$J = AE^2 \exp\left(-\frac{B\Phi_i^{-3/2}}{E}\right)$ [18], where A and B are constants, Φ_i is potential barrier height and E is the applied electric field.

Figure 4 shows the ferroelectric polarization vs. electric field (P–E) curves of the BFPT, BLFPT, BFMPT and BLFMPT thin films at RT with a measurement frequency of 1 kHz. The P–E loop of the BFPT film which contained some leakage current components is much more rounded than those of doped BFPT films. The film of BLFPT demonstrates the reduced coercive field and relatively saturated P–E hysteresis loops, while a degradation of remnant polarization is observed [19]. In addition, it can be found that the retention properties of the film has also deteriorated. The remnant polarization after 1 s of relaxation is close to 10 uC/cm^2, less than half of the sample that without La substitution. La^{+3} substitution for Bi^{+3} supposed to be an effective way to reduce bismuth vacancies that are accompanied by oxygen vacancies and thus decrease the film conductivity [20]. The decreased oxygen vacancies reduces the possibility of pinning of the domains and promotes the ferroelectric polarization. In this case, the more reversible domain leads to the decrease of coercive field. Nevertheless, it is also helpful for domains to turn back when the electric field is removed. It could be considered to be the reason for the degradation of polarization and retention in BLFPT film. Subsequently, due to the significant effects of Mn doping in improving the electrical resistivity, the BFMPT film displays the improved polarization with a better P–E loop. However, there is no significant decrease of coercive field. The BLFMPT film shows a highly desirable P–E loop ($P_r \sim 37$ uC/cm^2 and $E_c \sim 90$ kV/cm) for La and Mn co-substitution combines the advantages of La and Mn doping, except for retention performance is affected by La substitution. Indeed, as one of the causes for modified hysteresis loop, the lower leakage current of BLFMPT is already shown above of Fig. 3. Moreover, La substitution promote the domain's reversal, which further enhanced the polarization in Mn-doped BFPT film [17]. Accordingly, it can be inferred that homogeneous domains achieved via the La insertion, combines with significantly reduced leakage current in film by Mn substitution, which in turn lead to the enhanced ferroelectric properties.

4 Conclusions

We have synthesized La-doped and Mn-doped BFPT thin films by chemical solution deposition. It turned out that more homogeneous domains could be achieved by La substitution, which contribute to the promotion of domain's reversal. However, it simultaneously display a degradation of remnant polarization and retention property. Meanwhile, films of BFPMT demonstrated the enhanced insulation and improved polarization for Mn insertion. La and Mn co-substitution combined the advantages of La doping and Mn doping, which exhibited the lowest the leakage current in the measured electric field range. In addition, a well saturated P–E hysteresis loop ($P_r \sim 37$ uC/cm^2 and $E_c \sim 90$ kV /cm) of BLFPMT was achieved at room temperature with a measurement frequency of 1 kHz. In order to make the film available for practical application in the field of non-volatile memories, method for improving film retention characteristics will be investigated in the following work.

Acknowledgements This work was supported by the National Natural Science Foundation of China (Grant no.51302163) and the Innovational Foundation of Shanghai University (Grant. no. K.10-0110-13-009).

Compliance with ethical standards

Conflict of interest The authors declare that they have no competing interests.

References

1. Wang J, Neaton JB, Zheng H, Nagarajan V, Ogale SB, Liu B, Viehland D, Vaithyanathan V, Schlom DG, Waghmare UV, Spaldin NA, Rabe KM, Wuttig M, Ramesh R (2003) Science 299:1719–1722
2. Catalan G, Scott JF (2009) Adv Mater 21:2463–2485
3. Martin LW, Ramesh R (2012) Acta Mater 60:2449–2470
4. Khan MikaelA, Comyn TimP, Bell AndrewJ (2007) Appl Phys Lett 91:032901
5. Sakamoto Wataru, Iwata Asaki, Yogo Toshinobu (2008) J Appl Phys 104:104106
6. Zheng RY, Wang J, Ramakrishna S (2008) J Appl Phys 104:034106
7. Wu JG, Wang J (2010) Acta Mater 58:1688–1697
8. Katoch Rajesh, Gupta Rajeev, Garg Ashish (2014) Solid State Commun 177:103–107
9. Wu JG, Kang GQ, Liu HJ, Wang J (2009) Appl Phys Lett 94:172906
10. Wu JG, Kang GQ, Wang J (2009) Appl Phys Lett 95:192901
11. Zhu W-M, Ye Z-G (2006) Appl Phys Lett 89:232904
12. Kim Woo-Hee, Son JongYeog (2013) Appl Phys Lett 103:132907
13. Singh SK, Ishiwara H (2006) Appl Phys Lett 88:262908
14. Wu Jiagang, Wang John (2010) J Am Ceram Soc 93:2795–2803
15. Izumi Hirokazu, Yoshimura Takeshi, Fujimura Norifumi (2017) J Appl Phys 121:174102
16. Sun W, Zhou Z, Luo J, Wang K, Li JF (2017) J Appl Phys 121:064101
17. Yan F, Zhu TJ, Lai MO, Lu L (2010) Scr Mater 63:780–783
18. Xu Jianlong, Jia Ze, Zhang Naiwen, Ren Tianling (2012) J Appl Phys 111:074101
19. Wang Y, Zheng RY, Sim CH, Wang J (2009) J Appl Phys 105:016106
20. Simões AZ, Aguiar' EC, Gonzalez AHM, Andrés J, Longo E, Varela JA (2008) J Appl Phys 104:104115